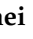*Article*

Approximating Helical Pile Pullout Resistance Using Metaheuristic-Enabled Fuzzy Hybrids

Mohammadmehdi Ahmadianroohbakhsh [1], Farzad Fahool [2], Mohammad Sadegh Saffari Pour [3], S. Farid F. Mojtahedi [4], Behnam Ghorbanirezaei [5] and Moncef L. Nehdi [6,*]

1 Department of Geotechnical Engineering, Estahban Branch, Islamic Azad University, Estahban 1477893855, Iran

2 Department of Mining Engineering, Amirkabir University of Technology, Tehran 1591634311, Iran

3 Department of Civil Engineering, Shahid Bahonar University, Kerman 7616913439, Iran

4 Department of Infrastructure Engineering, University of Melbourne, Melbourne 3010, Australia

5 Department of Civil Engineering, Islamic Azad University, Central Tehran Branch, Tehran 1477893855, Iran

6 Department of Civil Engineering, McMaster University, Hamilton, ON L8S 4L8, Canada

* Correspondence: nehdim@mcmaster.ca

Abstract: Piles have paramount importance for various structural systems in a wide scope of civil and geotechnical engineering works. Accurately predicting the pullout resistance of piles is critical for the long-term structural resilience of civil infrastructures. In this research, three sophisticated models are employed for precisely predicting the pullout resistance (P_{ul}) of helical piles. Metaheuristic schemes of gray wolf optimization (GWO), differential evolution (DE), and ant colony optimization (ACO) were deployed for tuning an adaptive neuro-fuzzy inference system (ANFIS) in mapping the P_{ul} behavior from three independent factors, namely the embedment ratio, the density class, and the ratio of the shaft base diameter to the shaft diameter. Based on the results, i.e., the Pearson's correlation coefficient (R = 0.99986 vs. 0.99962 and 0.99981) and root mean square error (RMSE = 7.2802 vs. 12.1223 and 8.5777), the GWO-ANFIS surpassed the DE- and ACO-based ensembles in the training phase. However, smaller errors were obtained for the DE-ANFIS and ACO-ANFIS in predicting the P_{ul} pattern. Overall, the results show that all three models are capable of predicting the P_{ul} for helical piles in both loose and dense soils with superior accuracy. Hence, the combination of ANFIS and the mentioned metaheuristic algorithms is recommended for real-world purposes.

Keywords: helical piles; pullout resistance; fuzzy systems; evolutionary optimization

1. Introduction

With recent advances in measuring technologies and computational methods, the world of engineering has experienced significant improvements [1–3]. These improvements comprise various domains, such as civil engineering and earth science [4,5], hydrology and water science [6], material assessment [7], etc. A more explicit example of the civil engineering field could be assessing concrete-based structural elements and their behavior under different loading conditions [8,9]. Focusing on geotechnical engineering, many scientists have employed analytical and numerical approaches for assessing various phenomena (e.g., rock mass movement [10], behavior of crystalline rock [11], etc.).

A primary purpose of the mentioned efforts has been to facilitate burdensome issues through employing computer-based software and algorithms [12,13]. The application of soft computing (SC) techniques has produced encouraging results in a wide variety of engineering domains [14–16]. Since geotechnical operations are the basis of many civil engineering projects, solving related problems has always been a vital and challenging task for engineers. Many scholars have profitably applied intelligent models to different geotechnical simulations, such as slope stability [17], soil shear strength [18], soil permeability [19], bearing capacity (BC) of foundations [20], etc. These studies, as well as

many similar efforts, have shown the suitability of data mining methods and argued their efficiency in comparison with traditional approaches.

A pile is a widely used form of foundation that has complicated calculations for analyzing different parameters. The SC-based methods have provided efficient solutions for predicting various parameters of piles (e.g., BC [21], drivability [22], and settlement [23]). These methods exploit particular strategies to comprehend the relationship between a set of dependent–independent factors. An artificial neural network (ANN) [24], for example, is an imitation of the biological neural system. Nguyen et al. [25] estimated the frictional resistance of driven piles using a four-layer ANN. Moayedi and Hayati [26] applied a feed-forward ANN to the information of bored piles for forecasting load–settlement responses. Their proposed model achieved an accuracy greater than 99% (in terms of the R-squared correlation index). A support vector machine (SVM) [27] is a statistic-based learner that has successfully performed many classification and regression simulations. Scholars, including Pal and Deswal [28] and Ghazanfari-Hashemi et al. [29], have used SVMs for predicting the capacity and group scour of piles.

The adaptive neuro-fuzzy inference system (ANFIS) is another potent processor that incorporates the ANN and fuzzy rules for non-linear analysis. This property has made the ANFIS a strong predictive tool. Zhang et al. [30] used this model for simulating the ultimate bearing capacity (UBC) of single piles. The quick convergence and large accuracy in reproducing an analyzed pattern were mentioned as the merits of the used ANFIS. Tien Bui et al. [31] showed the higher efficiency of ANFISs in comparison with three common notions of ANNs, namely feed-forward, radial basis functions, and general regression ANNs, in modeling the behavior of pullout resistance (P_{ul}) of belled piles. The variance account for (VAF) the statistical index was 97.442 and 96.247 for the training and prediction phases of the used ANFI, respectively. Ghorbani et al. [32] could predict the ultimate axial load BC with 96% accuracy by feeding an ANFIS based on the records from a cone penetration test (CPT). They obtained a tractable predictive equation from the suggested model.

Geotechnical scholars have also paid much attention to the recently developed metaheuristic science in their works [33,34]. Azimi et al. [35] proposed a hybrid of the ANFIS coupled with differential evolution (DE) and singular decomposition value (SVD) to model scour at pile groups. In addition to proving the applicability of the developed ANFIS-DE/SVD model, they showed its better performance in comparison with empirical approaches and genetic algorithms (GAs). Moayedi et al. [36] optimized an ANFIS using particle swarm optimization (PSO) and GA for forecasting the friction capacity ratios of driven shafts. They could reduce the root mean square error (RMSE) of the ANFIS from 0.0123 to 0.0119 and 0.0117. Thus, the GA-fuzzy model was introduced as the most reliable predictor. Harandizadeh et al. [37] synthesized a gravitational search algorithm and a group method of data handling with the ANFIS to approximate the pile BC. With an RMSE of 0.084, the proposed model outperformed the regression-based approaches.

In most previous efforts, the optimization of all intelligent models, including ANN and ANFIS, has been carried out by well-tried optimizer algorithms, such as the PSO, GA, etc. As a matter of fact, these algorithms belong to the initial notions of metaheuristic algorithms, while nowadays, complicated problems call for evaluating newer approaches to keep the solution updated with recent developments. Therefore, this research is conducted to audit the efficiency of three novel ANFIS-based hybrids in assessing the pullout resistance (P_{ul}) of helical piles. In spite of the broad applicability of metaheuristic schemes in analyzing the parameters of piles, the literature lacks efforts to employ fuzzy-metaheuristic techniques for the mentioned objective. Three metaheuristic optimizers—gray wolf optimization (GWO), differential evolution (DE), and ant colony optimization (ACO)—were used for tuning the parameters of ANFIS membership functions (MFs). The global search ability of these algorithms protects the ANFIS from possible computational drawbacks. A comparison was performed among the proposed models using various accuracy demonstrators, and the most effective model was introduced. As a potential contribution to the body of knowledge,

the models of this study can replace the costly and time-consuming traditional methods and the existing burdensome numerical approaches by efficiently analyzing the resistance of piles.

2. Materials and Methods

2.1. Data Provision

As with other geotechnical parameters, the P_{ul} is affected by different factors. When it comes to intelligent simulations, these effective factors play the role of inputs for a target parameter. It means that the network tries to map their relationship to capture a pattern. In the present attempt and based on the dataset provided by Nazir et al. [38], the input factors are the embedment ratio (L/D_b), the density class (DC), and the ratio of the shaft base diameter over the shaft diameter (D_b/D_s). This dataset has been used in a number of earlier papers [39,40]. Using 80% of the data for the training process is well accepted in machine learning implementation. The remaining 20% are, consequently, specified for the testing phase. Considering a total of 36 records in the dataset, 29 and 7 samples were randomly selected to analyze and generalize the P_{ul} behavior.

Figure 1 depicts the variations of 36 values for all four parameters. In Figure 1a, six values of 0, 1, 2, . . . , and 5 (each having a frequency of 6) are seen for the L/D_b. Figure 1b reports the presence of two soil categories, i.e., dense and loose soils, signified by DC values equal to 85 and 35, respectively. As for the D_b/D_s, three values of 0.3, 0.4, and 0.5 are repeated 12 times in Figure 1c. As Figure 1d displays, the P_{ul} values are fluctuating in an irregular pattern. For this parameter, the statistical indicators of mean, standard deviation, sample variance, minimum, and maximum equal 376.86, 465.09, 216,316.33, 0, and 1622.47, respectively.
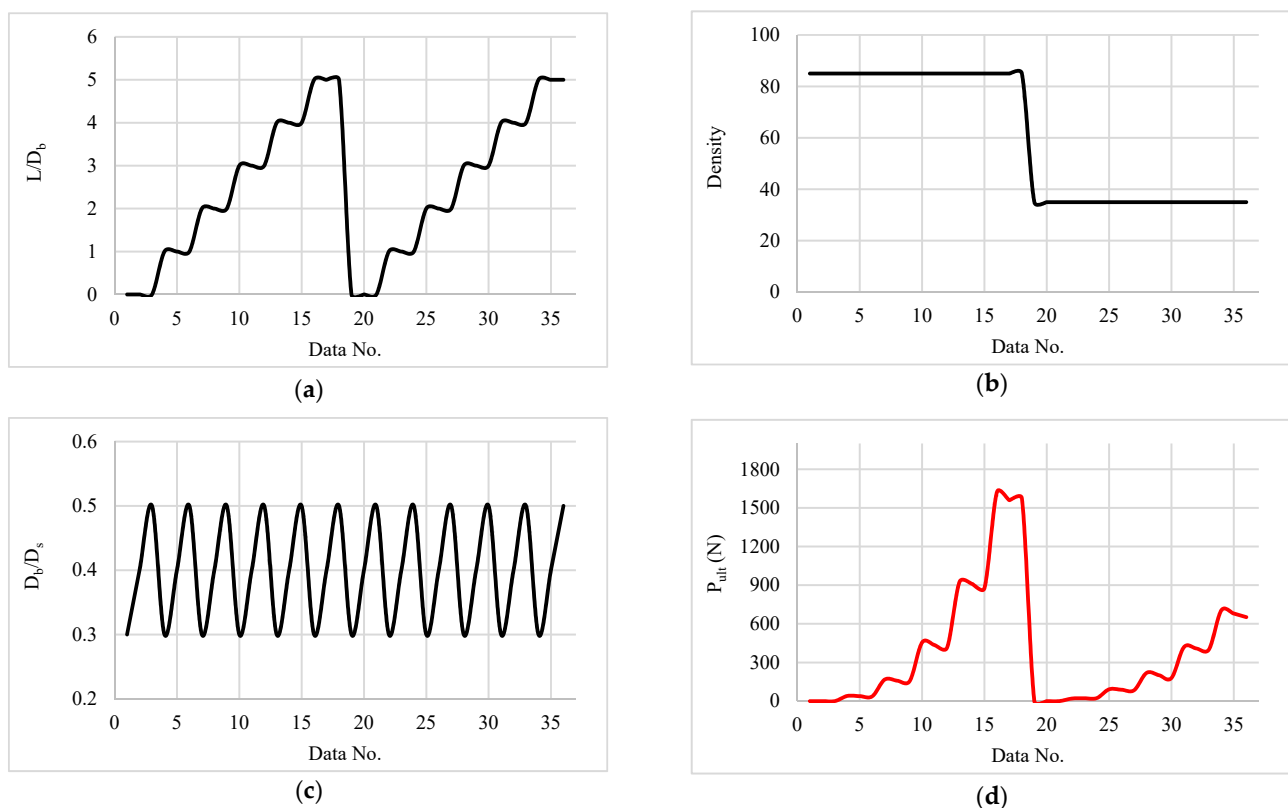
Figure 1. Variations in the (**a**–**c**) independent and (**d**) dependent parameters.

2.2. The ANFIS Model

Jang [41] combined the interpretability of a FIS with the learning strategy of an ANN to invent the ANFIS. Up to now, intelligent models including ANFIS have gained

increasing popularity for mapping highly non-linear problems, such as suspended sediment concentration [42], landslide susceptibility [43], soil shear strength [44], etc., from their specific factors.

Figure 2 depicts the configuration of a standard ANFIS, mapping the output Z from the inputs X and Y through five layers. Given that D_i and S_i are the fuzzy sets and p_i, q_i, and r_i are the output parameters, the below if–then regulations can be written as follows:

$$\text{Regulation 1}: \text{ If X is } D_1 \text{ and Y is } S_1, \text{ then } Z_1 = j_1 X + k_1 Y + l_1$$
$$\text{Regulation 2}: \text{ If X is } D_2 \text{ and Y is } S_2, \text{ then } Z_2 = j_2 X + k_2 Y + l_2$$
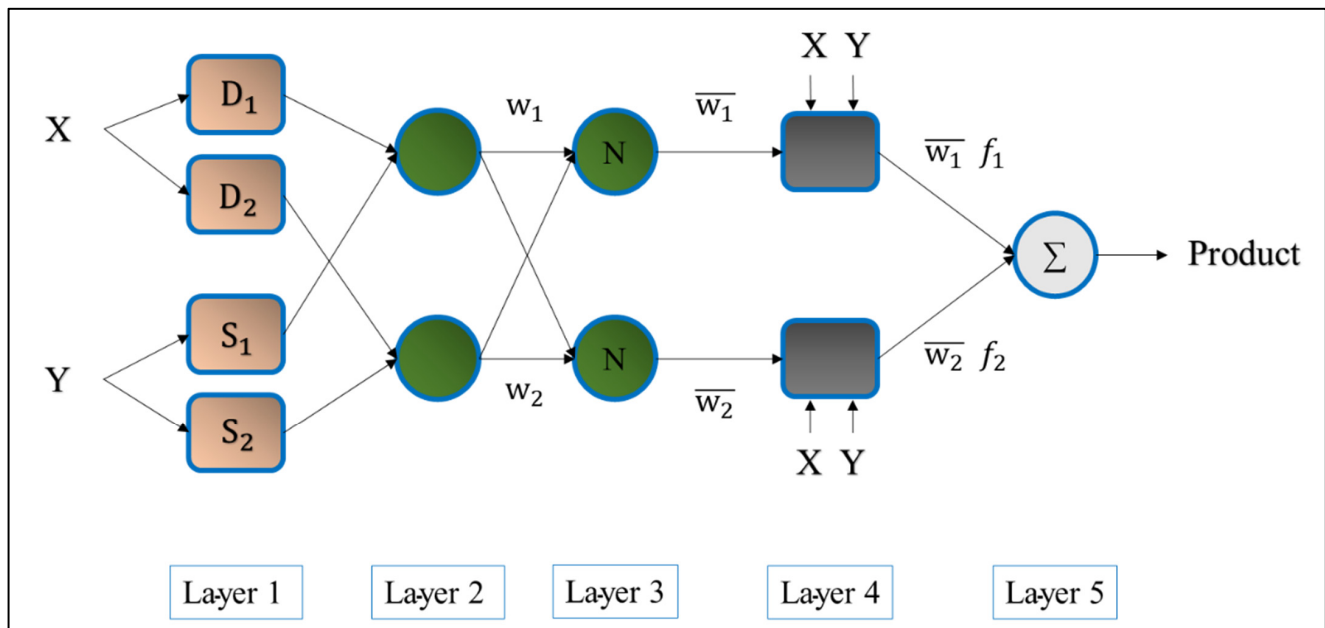
Figure 2. Schematic of a five-layer ANFIS structure.

The calculations of the illustrated five layers are presented in [45] (for two inputs) and as follows:

Layer 1: The MF values of the input variables are calculated as follows:

$$Q_{1,i} = \mu_{D_i}(X), \text{for} i = 1,\ 2,\ 3, \tag{1}$$

$$Q_{1,i} = \mu_{S_{i-3}}(Y), \text{for} i = 4,\ 5,\ 6, \tag{2}$$

where D_i and S_{i-3} are the MFs for the inputs.

Layer 2: The fixed nodes multiply the incoming signals, which is expressed as follows:

$$Q_{2,i} = w_i = \mu_{D_i}(X) \cdot \mu_{S_i}(Y), \quad i = 1,\ 2, \tag{3}$$

Layer 3: The normalized firing strength is produced as follows:

$$Q_{3,i} = \overline{w}_i = \frac{w_i}{w_1 + w_2}, \quad i = 1, 2, \tag{4}$$

Layer 4: Assuming j_i, k_i, and l_i are the consequent parameters, a linear combination is released as follows:

$$Q_{4,i} = \overline{w}_i\, f_i = \overline{w}_i\,(j_i X + k_i Y + l_i), \tag{5}$$

Layer 5: The overall response of the ANFIS is produced by the following relationship [46]:

$$Q_{5,i} = \sum \overline{w}_i\, f_i = \sum w_i f_i / \sum w_i, \tag{6}$$

2.3. The GWO, DE, and ACO Optimizers

According to many recent studies, metaheuristic algorithms open new doors to using artificial intelligence techniques in a more reliable way. They are able to retrofit these models by overcoming various computational drawbacks, such as local minima [47] and dimension danger [48]. They perform specific social/foraging search strategies to attain the universally optimal solution to a given problem.

Figure 3 displays an optimization procedure where the optimal configuration of the ANFIS is discovered by the GWO, DE, and ACO metaheuristic search methods. A new FIS is created in each iteration using the found solution. The quality of this solution is reflected by measuring the accuracy of the developed FIS. This process is detailed in the sections below.
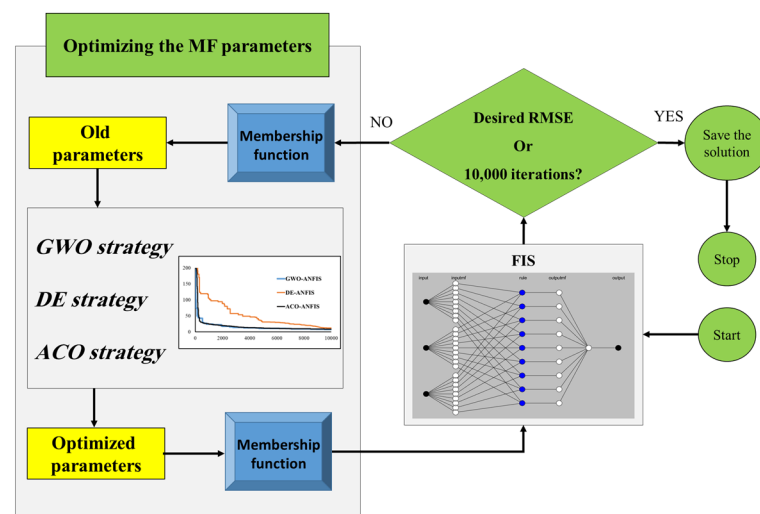

Figure 3. Schematic vision of the optimization procedure.

The optimization strategy of each algorithm is introduced in this section:

Mirjalili et al. [49] created the GWO by simulating the hunting strategy of a herd of gray wolves. This algorithm has been widely used for various optimization issues. Based on strict social rules of dominance, the wolves are classified into four groups, namely alpha, beta, delta, and omega, so that the alpha is the most powerful member and, consequently, the decision-maker of the herd. The alpha is assisted by beta members. As the subordinates of these two groups, delta wolves play the roles of scouts, sentinels, hunters, and caretakers. They also have to report their actions to the superior members. Omega wolves are the members with the least important roles, such as assisting and satisfying other members. The hunting process is expressed by the following three major steps: (a) tracking, chasing, and intimidating the prey by moving towards it; (b) encircling and harassing the hunt to immobilize it; (c) eventually hunting the prey down [50]. More details on the GWO can be found in the related literature [51–53].

Storn and Price [54] presented the DE as an efficient population-based heuristic method. This algorithm enjoys several advantages, including simplicity, ease of use, real coding, and speed. The main rules are established for two sets of a population, namely the old and new generations of one population. There are several real-valued vectors with dimension D (equaling the number of control parameters) in the population. The bounds of the initial parameters are considered to randomly initialize the population. The three major operations implemented during the optimization process are as follows: (i) mutation; (ii) crossover; (iii) selection. The members of the present society of each generation become target vectors, and a mutant vector is generated for each one. To perform this, the weighted difference between two randomly selected vectors is added to a third vector. The operators of the crossover mix the parameters of the target and mutant vectors to produce the so-called "trial vector". The fitness of the trail and target vectors are compared together

to determine the necessity of replacing the target vector in the future generation [55]. For further information on the DE, please refer to [56,57].

Inspired by the cooperative food-seeking behavior of ants, the ACO was designed by Dorigo et al. [58] as a robust optimizer. It has been widely applied to many discrete optimization problems in different domains. The ACO treats a problem as a weighted graph and aims to find the optimal path on it. In the initial step, a number of ants move in randomly chosen directions relative to their nest to seek nectar. They mark any path they take by producing a chemical substance called a pheromone. Once one nectar is detected, the discoverer ant takes a portion of the food and returns to the nest via the path distinguished by the greatest amount of pheromones. The searching process is started again from the nest to find more promising paths. It updates the solution to the problem. The optimal solution is finally determined by the shortest path, which always contains the greatest pheromone trail [59]. Due to utilizing a distributed long-term memory for keeping previously obtained knowledge and a greedy strategy in the algorithm, the ACO can strongly perform both global and local searches. Studies such as [60,61] have presented further details about the ACO technique.

3. Results and Discussion

As denoted in the introduction, this study is dedicated to evaluating three fuzzy-metaheuristic hybrids in simulating the P_{ul} of helical piles. As with any prediction problem, the results are compared to the expected values to measure the accuracy of the models. To this end, the Pearson's correlation coefficient (R), mean absolute error (MAE), and root mean square error (RMSE) are used to report the correlation and error of the results based on the following formulations:

$$R = \frac{\sum\limits_{i=1}^{G} \left(P_{ul i_{predicted}} - \overline{P_{ul}}_{predicted}\right)\left(P_{ul i_{observed}} - \overline{P_{ul}}_{observed}\right)}{\sqrt{\sum\limits_{i=1}^{G} \left(P_{ul i_{predicted}} - \overline{P_{ul}}_{predicted}\right)^2}\sqrt{\sum\limits_{i=1}^{G} \left(P_{ul i_{observed}} - \overline{P_{ul}}_{observed}\right)^2}}, \qquad (7)$$

$$MAE = \frac{1}{G}\sum\limits_{i=1}^{G}\left|P_{ul i_{laboratory}} - P_{ul i_{simulated}}\right|, \qquad (8)$$

$$RMSE = \sqrt{\frac{1}{G}\sum\limits_{i=1}^{G}\left[\left(P_{ul i_{laboratory}} - P_{ul i_{simulated}}\right)\right]^2}, \qquad (9)$$

where $P_{ul_{i\ simulated}}$ and $P_{ul_{i\ laboratory}}$ signify the estimated and experimental P_{ul}s, respectively.

3.1. Optimization and Convergence

After assigning the metaheuristic optimizers for tuning the parameters in the MFs, three hybrids of GWO-ANFIS, DE-ANFIS, and ACO-ANFIS were created. Since a stochastic strategy is applied by these algorithms, they need a sufficient number of iterations to approach the most optimal solutions. Unlike many previous studies that have bound this parameter to common values (such as 1000 iterations) [62,63], exploring the convergence paths of all three ANFISs showed that they can be further optimized if larger numbers are considered for the iterations of GWO, DE, and ACO. Hence, by taking 10,000 iterations, the algorithms could attain a suitable level of accuracy. Figure 4 shows the convergence curves of the implemented models, where the RMSE plays the role of the OF. Notably, the population sizes of the GWO-ANFIS, DE-ANFIS, and ACO-ANFIS were 200, 10, and 5, respectively.
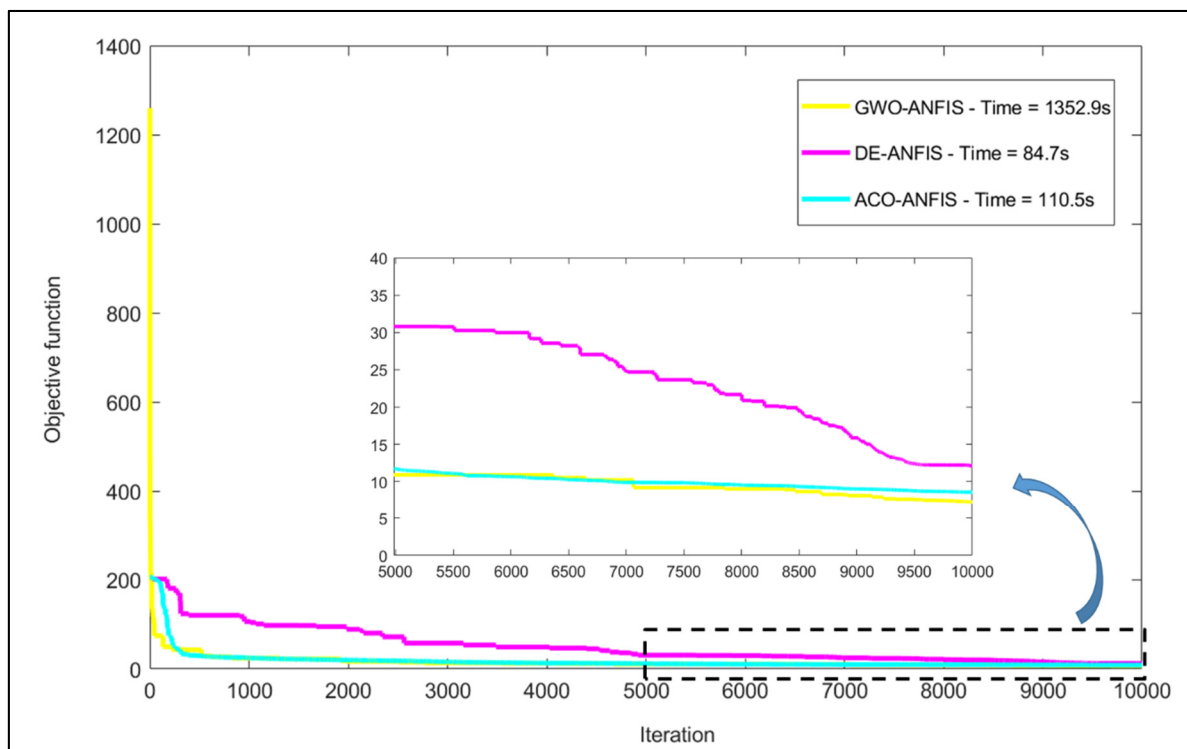
Figure 4. Comparing the optimization curves of the metaheuristic-trained fuzzy tools.

According to the above figure, the curve of the GWO starts at 1259.5107 and ends at 7.2801. This is while both the DE and ACO started with 204.3240 and reached 12.1223 and 8.5777 at the end, respectively. The magnified segment reveals the behavior of each curve for the second 5000 iterations. It can be seen that the GWO finally won a close competition with the ACO.

3.2. Training and Testing Results and Comparison

The low values of RMSE (7.2802, 12.1223, and 8.5777 for the GWO-ANFIS, DE-ANFIS, and ACO-ANFIS, respectively) obtained during the optimization process indicated that all three models have performed successfully in recognizing the P_{ul} behavior. Figure 5 depicts the actual P_{ul}s versus the corresponding predicted values. As it can be seen, these models have correctly predicted the changes in the target parameters. Additionally, the drawn pattern is highly adaptable and difficult to distinguish. This is why the two critical sections are magnified to better illustrate the comparison. The models have presented a close prediction in these figures. However, the line of the GWO-ANFIS is more compatible with the target values. The MEAs obtained for all 29 training samples were 6.4980, 8.6465, and 6.5006, which confirms the larger error of the DE-ANFIS.

Assessing the models using the seven testing samples revealed that all trained ANFISs can popularize the inferred P_{ul} behavior to unseen conditions. Figure 6 depicts the errors (= $P_{ul_i \ laboratory} - P_{ul_i \ simulated}$) for these samples. Compared to the training phase, larger error indicators (RMSEs of 26.4759, 20.4362, and 16.9520 and MAEs of 14.3905, 13.2905, and 13.8824) were obtained for this phase.
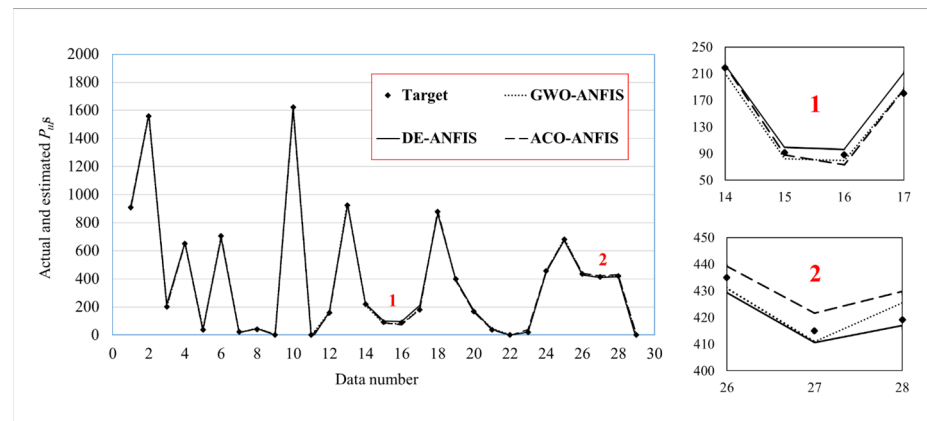
**Figure 5.** Pattern comparison for the training samples.
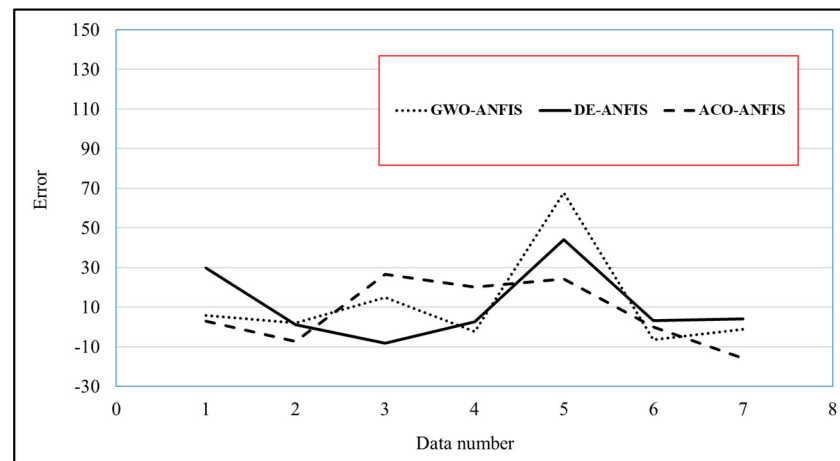
Figure 6. Simple errors calculated for the testing samples.

To provide a visual correlation between the laboratory and predicted P_{ul}s, Figure 7 shows the regression charts of the GWO-ANFIS, DE-ANFIS, and ACO-ANFIS. The calculated correlation indices (i.e., R) were 0.99986, 0.99962, and 0.99981 for the training data and 0.99978, 0.99973, and 0.99967 for the testing data. A correlation of more than 99.9% for the stages confirms the capability of the used hybrid tools in predicting the P_{ul} as a vital geotechnical parameter.

The contents of the below figures compare the results for specific conditions of the problem. Figure 8 plots the target parameter versus D_b/D_s, where L/D_b equals 1 (for dense soils) and 4 (for loose soils). It can be seen that the pullout resistance of the pile decreases with the degradation of D_b/D_s. The same behavior is observed in patterns generated by the GWO-AFNIS, DE-ANFIS, and ACO-AFNIS. This, once again, confirms the high accuracy of the developed models for predicting the P_{ul}. For instance, for the pile in loose soil with an embedment ratio = 4 and a D_b/D_s ratio = 0.4, the $P_{ul} = 408.51$ has been predicted to be 415.11, 405.33, and 408.43.

Similarly, Figure 9 plots the P_{ul} versus L/D_b, where D_b/D_s equals 0.3 (for dense soils) and 0.5 (for loose soils). As is obvious, the increasing trends of the target parameter have been correctly simulated by the applied models for both loose and dense soils.
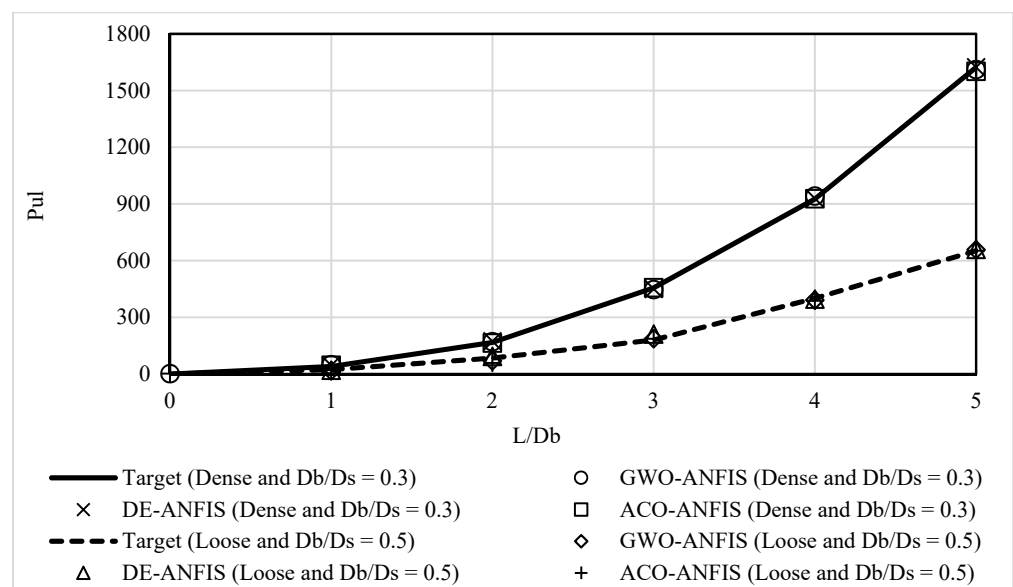
(**a**)

(**b**)

(**c**)

(**d**)

(**e**)

(**f**)
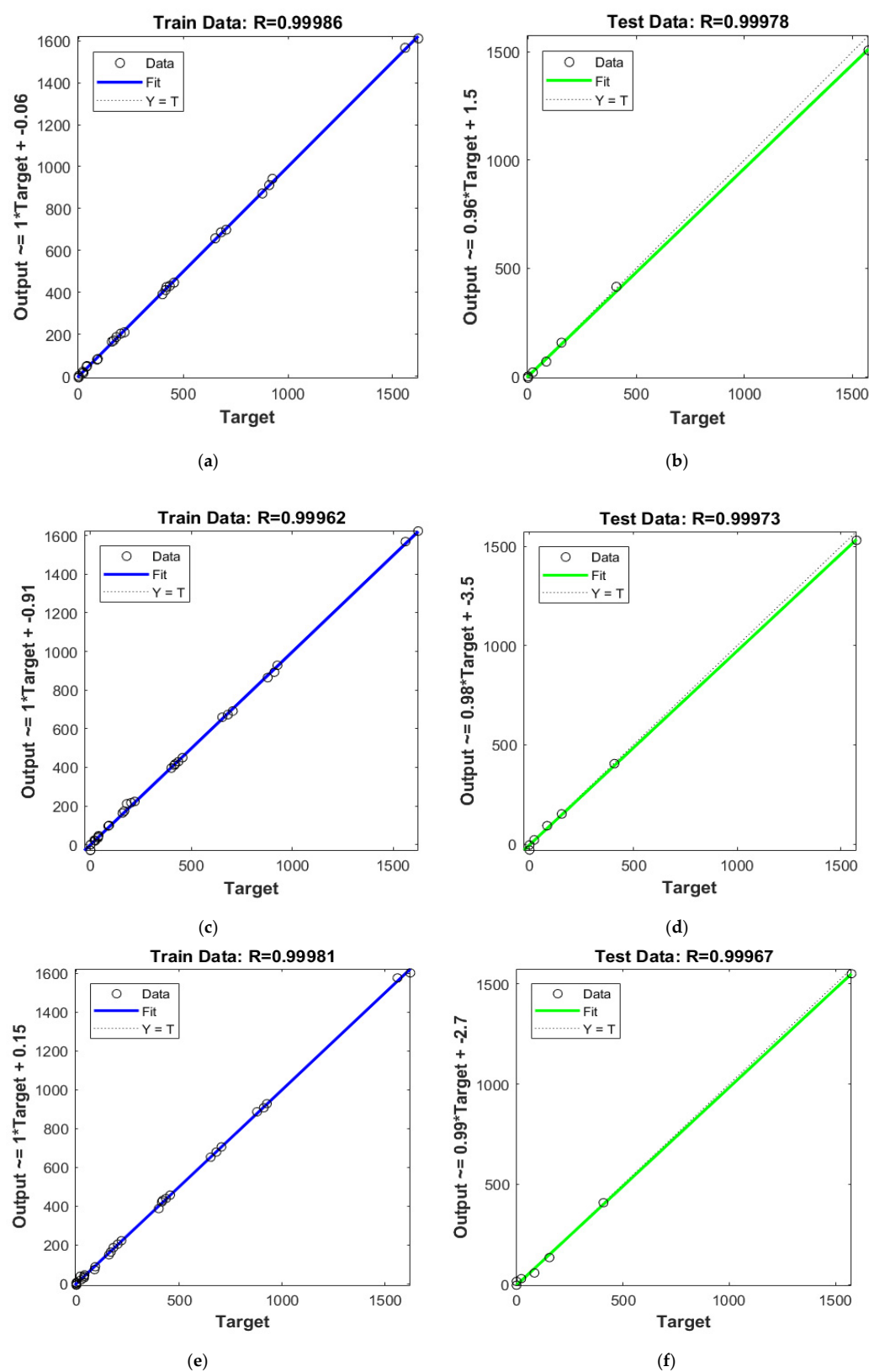
Figure 7. Regression charts for the training and testing results of (**a**,**b**) GWO-ANFIS, (**c**,**d**) DE-ANFIS, and (**e**,**f**) ACO-ANFIS.
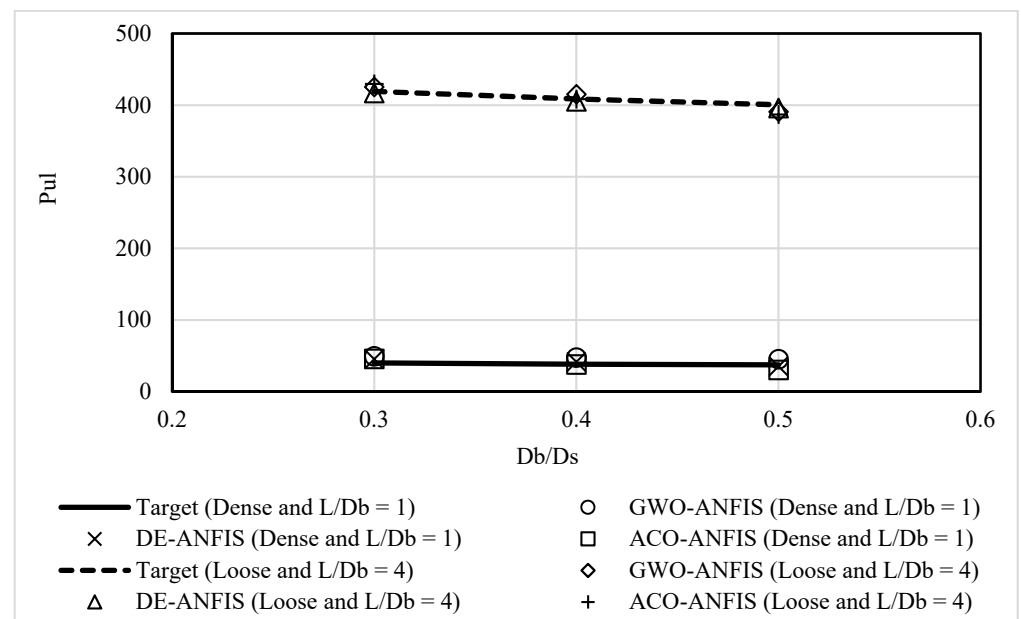
Figure 8. An example of the P_{ul} values versus the D_b/D_s ratio.

Figure 9. An example of the P_{ul} values versus the L/D_b ratio.

Moreover, the accuracy evaluations indicated that there are noticeable differences between the performances of the models. All three accuracy indicators demonstrated the superiority of the GWO in training the ANFIS model. The ACO, however, presented a very close performance as the second-best metaheuristic algorithm.

The prediction accuracies measured in the testing phase raised disagreements with the learning quality of the models. The best results were indicated by the RMSE = 16.9520, MAE = 13.2905, and R = 0.99978, which were obtained for the GWO-AFNIS, DE-ANFIS, and ACO-AFNIS, respectively. In addition, due to the second position of the DE-ANFIS in terms of the RMSE and R indices, it may be the most accurate hybrid in predicting the P_{ul}.

3.3. Further Discussion

Geotechnical engineering has experienced notable advances with reference to recent achievements [64,65]. Piles are fundamental geotechnical elements that are being used worldwide. Engineers have tried different approaches (e.g., numerical, analytical, etc.) to

capture an estimation of the behavior of piles, which leads to more effective designs [66,67]. With the advent of machine learning tools, they have received high attention for predicting the parameters of piles [68]. In this sense, metaheuristic algorithms have assisted normal machine learning in carrying out non-linear analysis.

This work proposed and evaluated the effectiveness of three ANFIS-based approaches for estimating the P_{ul}, which is a significant parameter of piles. The used algorithms, i.e., DE, GWO, and ACO, could nicely optimize the ANFIS internal configuration and establish a network for predicting this parameter. Although the models performed differently in terms of various accuracy indicators, they are all suitable and accurate approaches for this task.

Although DE-ANFIS was considered more accurate than the two other methods, referring to Figure 4, this algorithm requires a much larger number of iterations to reach a suitable accuracy. Hence, the use of ACO and GWO may be preferred for time-sensitive applications, as these algorithms could reach a desirable accuracy with around 1000 iterations.

From a practical perspective, the offered methods can be reliably used for analyzing the resistance of piles for real-world projects. This generalizability is based on the excellent performance of the models for testing data that represent unseen new conditions for both soil types (i.e., loose and dense). As illustrated in Figures 8 and 9, the behavior of the pile can be well predicted only by receiving three characteristics, including L/D_b, DC, and D_b/D_s. Such an understanding has two major benefits. First, it enables engineers to enhance early designs by trying possible conditions. Second, it can remove the need to perform burdensome traditional simulation methods, such as finite element and numerical techniques.

However, some viable ideas can be considered for future studies to enhance the discovered solutions. For instance, trying a larger and newer collection of metaheuristic algorithms along with basic methods, such as ANN and SVM, can broaden the variety of methods, each tailored for a specific condition. Besides, working on data (e.g., optimizing the number of input parameters) can lead to a more efficient network with lighter computations [69].

4. Conclusions

In order to surmount the computational drawbacks of the classical ANFIS, three automatic search techniques, namely gray wolf optimization, differential evolution, and ant colony optimization, were successfully used to adjust the parameters embedded in the MFs of this network.

Thus, hybrids of GWO-ANFIS, DE-ANFIS, and ACO-ANFIS were created and performed to approximate the pullout resistance for helical piles. After an extensive optimization process, it was shown that all three algorithms can grasp a precise understanding of the P_{ul} behavior. The RMSE of the GWO-ANFIS was 4.8421 and 1.2975 less than that of the DE-ANFIS and ACO-ANFIS, respectively.

With reference to the accuracy indicators in the testing phase, close predictions were presented by the models so that the smallest RMSE (16.9520), the smallest MAE (13.2905), and the largest R (0.99978) were obtained by the ACO-ANFIS, DE-ANFIS, and GWO-ANFIS, respectively. Overall, apart from the ranking, the results show the competency of the proposed models for estimating the P_{ul}, which warrants further investigation of their use in full-scale predictions in construction to explore the need for further refinement or extension beyond the capabilities of the current database used in the model development.

References

1. Li, S.; Geng, Z. Bicriteria scheduling on an unbounded parallel-batch machine for minimizing makespan and maximum cost. *Inf. Process. Lett.* **2023**, *180*, 106343. [CrossRef]
2. Zhang, C.; Kordestani, H.; Shadabfar, M. A combined review of vibration control strategies for high-speed trains and railway infrastructures: Challenges and solutions. *J. Low Freq. Noise Vib. Act. Control.* **2022**, 14613484221128682. [CrossRef]
3. Zhang, X.; Ma, F.; Dai, Z.; Wang, J.; Chen, L.; Ling, H.; Soltanian, M.R. Radionuclide transport in multi-scale fractured rocks: A review. *J. Hazard. Mater.* **2021**, *424*, 127550. [CrossRef]
4. Wang, G.; Zhao, B.; Wu, B.; Wang, M.; Liu, W.; Zhou, H.; Zhang, C.; Wang, Y.; Han, Y.; Xu, X. Research on the Macro-Mesoscopic Response Mechanism of Multisphere Approximated Heteromorphic Tailing Particles. *Lithosphere* **2022**, *2022*, 1977890. [CrossRef]
5. Zhang, Z.; Li, W.; Yang, J. Analysis of stochastic process to model safety risk in construction industry. *J. Civ. Eng. Manag.* **2021**, *27*, 87–99. [CrossRef]
6. Bai, B.; Rao, D.; Chang, T.; Guo, Z. A nonlinear attachment-detachment model with adsorption hysteresis for suspension-colloidal transport in porous media. *J. Hydrol.* **2019**, *578*, 124080. [CrossRef]
7. Shi, T.; Liu, Y.; Hu, Z.; Cen, M.; Zeng, C.; Xu, J.; Zhao, Z. Deformation Performance and Fracture Toughness of Carbon-Nanofiber-Modified Cement-Based Materials. *ACI Mater. J.* **2022**, *119*, 119–128. [CrossRef]
8. Huang, Y.; Zhang, W.; Liu, X. Assessment of Diagonal Macrocrack-Induced Debonding Mechanisms in FRP-Strengthened RC Beams. *J. Compos. Constr.* **2022**, *26*, 04022056. [CrossRef]
9. Shi, T.; Liu, Y.; Zhao, X.; Wang, J.; Zhao, Z.; Corr, D.J.; Shah, S.P. Study on mechanical properties of the interfacial transition zone in carbon nanofiber-reinforced cement mortar based on the PeakForce tapping mode of atomic force microscope. *J. Build. Eng.* **2022**, *61*, 105248. [CrossRef]
10. Guo, Y.; Luo, L.; Wang, C. Research on Fault Activation and Its Influencing Factors on the Barrier Effect of Rock Mass Movement Induced by Mining. *Appl. Sci.* **2023**, *13*, 651. [CrossRef]
11. Peng, J.; Xu, C.; Dai, B.; Sun, L.; Feng, J.; Huang, Q. Numerical Investigation of Brittleness Effect on Strength and Microcracking Behavior of Crystalline Rock. *Int. J. Géoméch.* **2022**, *22*, 04022178. [CrossRef]
12. Huang, H.; Li, M.; Yuan, Y.; Bai, H. Theoretical analysis on the lateral drift of precast concrete frame with replaceable artificial controllable plastic hinges. *J. Build. Eng.* **2022**, *62*, 105386. [CrossRef]
13. Huang, H.; Li, M.; Yuan, Y.; Bai, H. Experimental Research on the Seismic Performance of Precast Concrete Frame with Replaceable Artificial Controllable Plastic Hinges. *Eng. Struct.* **2023**, *149*, 04022222. [CrossRef]
14. Zhan, C.; Dai, Z.; Soltanian, M.R.; de Barros, F.P.J. Data-Worth Analysis for Heterogeneous Subsurface Structure Identification with a Stochastic Deep Learning Framework. *Water Resour. Res.* **2022**, *58*, e2022WR033241. [CrossRef]
15. Wang, G.; Zhao, B.; Wu, B.; Zhang, C.; Liu, W. Intelligent prediction of slope stability based on visual exploratory data analysis of 77 in situ cases. *Int. J. Min. Sci. Technol.* **2022**. [CrossRef]
16. ur Rehman, Z.; Khalid, U.; Ijaz, N.; Mujtaba, H.; Haider, A.; Farooq, K.; Ijaz, Z. Machine learning-based intelligent modeling of hydraulic conductivity of sandy soils considering a wide range of grain sizes. *Eng. Geol.* **2022**, *311*, 106899. [CrossRef]
17. Tien Bui, D.; Moayedi, H.; Gör, M.; Jaafari, A.; Foong, L.K. Predicting Slope Stability Failure through Machine Learning Paradigms. *ISPRS Int. J. Geo-Inf.* **2019**, *8*, 395. [CrossRef]
18. Ly, H.-B.; Pham, B.T. Prediction of Shear Strength of Soil Using Direct Shear Test and Support Vector Machine Model. *Open Constr. Build. Technol. J.* **2020**, *14*, 268–277. [CrossRef]
19. Singh, V.K.; Kumar, D.; Kashyap, P.; Singh, P.K.; Kumar, A.; Singh, S.K. Modelling of soil permeability using different data driven algorithms based on physical properties of soil. *J. Hydrol.* **2020**, *580*, 124223. [CrossRef]
20. Padmini, D.; Ilamparuthi, K.; Sudheer, K. Ultimate bearing capacity prediction of shallow foundations on cohesionless soils using neurofuzzy models. *Comput. Geotech.* **2008**, *35*, 33–46. [CrossRef]
21. Lee, I.-M.; Lee, J.-H. Prediction of pile bearing capacity using artificial neural networks. *Comput. Geotech.* **1996**, *18*, 189–200. [CrossRef]
22. Zhang, W.; Goh, A.T. Multivariate adaptive regression splines and neural network models for prediction of pile drivability. *Geosci. Front.* **2016**, *7*, 45–52. [CrossRef]
23. Baziar, M.H.; Aziakandi, A.S.; Kashkooli, A. Prediction of pile settlement based on cone penetration test results: An ANN approach. *KSCE J. Civ. Eng.* **2015**, *19*, 98–106. [CrossRef]

24. Zhang, L.; Zhang, B. A geometrical representation of McCulloch-Pitts neural model and its applications. *IEEE Trans. Neural Netw.* **1999**, *10*, 925–929. [CrossRef] [PubMed]

25. Nguyen, T.-A.; Ly, H.-B.; Jaafari, A.; Pham, T.B. Estimation of friction capacity of driven piles in clay using artificial Neural Network. *J. Sci. Earth* **2020**, *42*, 265–275. [CrossRef]

26. Moayedi, H.; Hayati, S. Applicability of a CPT-based neural network solution in predicting load-settlement responses of bored pile. *Int. J. Geomech.* **2018**, *18*, 06018009. [CrossRef]

27. Vapnik, V. *The Nature of Statistical Learning Theory*; Springer Science & Business Media: Berlin/Heidelberg, Germany, 2013.

28. Pal, M.; Deswal, S. Modeling Pile Capacity Using Support Vector Machines and Generalized Regression Neural Network. *J. Geotech. Geoenviron. Eng.* **2008**, *134*, 1021–1024. [CrossRef]

29. Ghazanfari-Hashemi, S.; Etemad-Shahidi, A.; Kazeminezhad, M.H.; Mansoori, A.R. Prediction of pile group scour in waves using support vector machines and ANN. *J. Hydroinform.* **2011**, *13*, 609–620. [CrossRef]

30. Zhang, Z.; Ding, D.; Rao, L.; Bi, Z. An ANFIS based approach for predicting the ultimate bearing capacity of single piles. In *Foundation Analysis and Design: Innovative Methods*; American Society of Civil Engineers: Reston, VA, USA, 2006; pp. 159–166.

31. Bui, D.T.; Moayedi, H.; Abdullahi, M.M.; Rashid, A.S.A.; Nguyen, H. Prediction of Pullout Behavior of Belled Piles through Various Machine Learning Modelling Techniques. *Sensors* **2019**, *19*, 3678. [CrossRef]

32. Ghorbani, B.; Sadrossadat, E.; Bazaz, J.B.; Oskooei, P.R. Numerical ANFIS-Based Formulation for Prediction of the Ultimate Axial Load Bearing Capacity of Piles Through CPT Data. *Geotech. Geol. Eng.* **2018**, *36*, 2057–2076. [CrossRef]

33. Foong, L.K.; Moayedi, H.; Lyu, Z. Computational modification of neural systems using a novel stochastic search scheme, namely evaporation rate-based water cycle algorithm: An application in geotechnical issues. *Eng. Comput.* **2020**, *37*, 3347–3358. [CrossRef]

34. Mehrabi, M.; Moayedi, H. Landslide susceptibility mapping using artificial neural network tuned by metaheuristic algorithms. *Environ. Earth Sci.* **2021**, *80*, 804. [CrossRef]

35. Azimi, H.; Bonakdari, H.; Ebtehaj, I.; Talesh, S.H.A.; Michelson, D.G.; Jamali, A. Evolutionary Pareto optimization of an ANFIS network for modeling scour at pile groups in clear water condition. *Fuzzy Sets Syst.* **2017**, *319*, 50–69. [CrossRef]

36. Moayedi, H.; Raftari, M.; Sharifi, A.; Jusoh, W.A.W.; Rashid, A.S.A. Optimization of ANFIS with GA and PSO estimating α ratio in driven piles. *Eng. Comput.* **2020**, *36*, 227–238. [CrossRef]

37. Harandizadeh, H.; Toufigh, M.M.; Toufigh, V. Application of improved ANFIS approaches to estimate bearing capacity of piles. *Soft Comput.* **2019**, *23*, 9537–9549. [CrossRef]

38. Nazir, R.; Chuan, H.S.; Niroumand, H.; Kassim, K.A. Performance of single vertical helical anchor embedded in dry sand. *Measurement* **2014**, *49*, 42–51. [CrossRef]

39. Wang, B.; Moayedi, H.; Nguyen, H.; Foong, L.K.; Rashid, A.S.A. Feasibility of a novel predictive technique based on artificial neural network optimized with particle swarm optimization estimating pullout bearing capacity of helical piles. *Eng. Comput.* **2019**, *36*, 1315–1324. [CrossRef]

40. Mosallanezhad, M.; Moayedi, H. Developing hybrid artificial neural network model for predicting uplift resistance of screw piles. *Arab. J. Geosci* **2017**, *10*, 479. [CrossRef]

41. Jang, J.-S.R. ANFIS: Adaptive-Network-Based Fuzzy Inference System. *IEEE Trans. Syst. Man Cybern.* **1993**, *23*, 665–685. [CrossRef]

42. Kisi, O. Suspended sediment estimation using neuro-fuzzy and neural network approaches/Estimation des matières en suspension par des approches neurofloues et à base de réseau de neurones. *Hydrol. Sci. J.* **2005**, *50*, 1–696. [CrossRef]

43. Mehrabi, M.; Pradhan, B.; Moayedi, H.; Alamri, A. Optimizing an Adaptive Neuro-Fuzzy Inference System for Spatial Prediction of Landslide Susceptibility Using Four State-of-the-art Metaheuristic Techniques. *Sensors* **2020**, *20*, 1723. [CrossRef] [PubMed]

44. Besalatpour, A.; Hajabbasi, M.A.; Ayoubi, S.; Afyuni, M.; Jalalian, A.; Schulin, R. Soil shear strength prediction using intelligent systems: Artificial neural networks and an adaptive neuro-fuzzy inference system. *Soil Sci. Plant Nutr.* **2012**, *58*, 149–160. [CrossRef]

45. Nauck, D.; Klawonn, F.; Kruse, R. *Foundations of Neuro-Fuzzy Systems*; John Wiley & Sons, Inc.: Hoboken, NJ, USA, 1997.

46. Çakıt, E.; Olak, A.J.; Karwowski, W.; Marek, T.; Hejduk, I.; Taiar, R. Assessing safety at work using an adaptive neuro-fuzzy inference system (ANFIS) approach aided by partial least squares structural equation modeling (PLS-SEM). *Int. J. Ind. Ergon.* **2020**, *76*, 102925. [CrossRef]

47. Moayedi, H.; Mehrabi, M.; Mosallanezhad, M.; Rashid, A.S.A.; Pradhan, B. Modification of landslide susceptibility mapping using optimized PSO-ANN technique. *Eng. Comput.* **2019**, *35*, 967–984. [CrossRef]

48. Moayedi, H.; Mehrabi, M.; Bui, D.T.; Pradhan, B.; Foong, L.K. Fuzzy-metaheuristic ensembles for spatial assessment of forest fire susceptibility. *J. Environ. Manag.* **2020**, *260*, 109867. [CrossRef]

49. Mirjalili, S.; Mirjalili, S.M.; Lewis, A. Grey wolf optimizer. *Adv. Eng. Softw.* **2014**, *69*, 46–61. [CrossRef]

50. Himanshu, N.; Kumar, V.; Burman, A.; Maity, D.; Gordan, B. Grey wolf optimization approach for searching critical failure surface in soil slopes. *Eng. Comput.* **2020**, *37*, 2059–2072. [CrossRef]

51. Kalemci, E.N.; Ikizler, S.B.; Dede, T.; Angın, Z. Design of reinforced concrete cantilever retaining wall using Grey wolf optimization algorithm. *Structures* **2019**, *23*, 245–253. [CrossRef]

52. Liao, K.; Wu, Y.; Miao, F.; Li, L.; Xue, Y. Using a kernel extreme learning machine with grey wolf optimization to predict the displacement of step-like landslide. *Bull. Eng. Geol. Environ.* **2020**, *79*, 673–685. [CrossRef]

53. Deng, S.; Wang, X.; Zhu, Y.; Lv, F.; Wang, J. Hybrid Grey Wolf Optimization Algorithm–Based Support Vector Machine for Groutability Prediction of Fractured Rock Mass. *J. Comput. Civ. Eng.* **2019**, *33*, 04018065. [CrossRef]

54. Storn, R.; Price, K. Differential evolution—A simple and efficient heuristic for global optimization over continuous spaces. *J. Glob. Optim.* **1997**, *11*, 341–359. [CrossRef]

55. Behera, A.; Panda, S.; Prakash, T.; Biswal, S. Design and performance analysis of a PID controller by using Differential Evolutionary Algorithm for an Autonomous Power System. *Int. J. Adv. Electr. Electron. Eng.* **2013**, *2*, 256–264.

56. Wang, C.; Liu, Y.; Zhang, Q.; Guo, H.; Liang, X.; Chen, Y.; Xu, M.; Wei, Y. Association rule mining based parameter adaptive strategy for differential evolution algorithms. *Expert Syst. Appl.* **2019**, *123*, 54–69. [CrossRef]

57. Zhang, Q.; Zou, D.; Duan, N.; Shen, X. An adaptive differential evolutionary algorithm incorporating multiple mutation strategies for the economic load dispatch problem. *Appl. Soft Comput.* **2019**, *78*, 641–669. [CrossRef]

58. Dorigo, M.; Birattari, M.; Stutzle, T. Ant colony optimization. *IEEE Comput. Intell. Mag.* **2006**, *1*, 28–39. [CrossRef]

59. Qamhan, A.A.; Ahmed, A.; Al-Harkan, I.M.; Badwelan, A.; Al-Samhan, A.M.; Hidri, L. An Exact Method and Ant Colony Optimization for Single Machine Scheduling Problem with Time Window Periodic Maintenance. *IEEE Access* **2020**, *8*, 44836–44845. [CrossRef]

60. Parvin, H.; Moradi, P.; Esmaeili, S. TCFACO: Trust-aware collaborative filtering method based on ant colony optimization. *Expert Syst. Appl.* **2019**, *118*, 152–168. [CrossRef]

61. Luan, J.; Yao, Z.; Zhao, F.; Song, X. A novel method to solve supplier selection problem: Hybrid algorithm of genetic algorithm and ant colony optimization. *Math. Comput. Simul.* **2019**, *156*, 294–309. [CrossRef]

62. Termeh, S.V.R.; Kornejady, A.; Pourghasemi, H.R.; Keesstra, S. Flood susceptibility mapping using novel ensembles of adaptive neuro fuzzy inference system and metaheuristic algorithms. *Sci. Total. Environ.* **2018**, *615*, 438–451. [CrossRef]

63. Moayedi, H.; Mehrabi, M.; Kalantar, B.; Mu'Azu, M.A.; Rashid, A.S.A.; Foong, L.K.; Nguyen, H. Novel hybrids of adaptive neuro-fuzzy inference system (ANFIS) with several metaheuristic algorithms for spatial susceptibility assessment of seismic-induced landslide. *Geomat. Nat. Hazards Risk* **2019**, *10*, 1879–1911. [CrossRef]

64. Zhang, Z.; Liang, G.; Niu, Q.; Wang, F.; Chen, J.; Zhao, B.; Ke, L. A Wiener degradation process with drift-based approach of determining target reliability index of concrete structures. *Qual. Reliab. Eng. Int.* **2022**, *38*, 3710–3725. [CrossRef]

65. Zhang, C.; Ali, A. The advancement of seismic isolation and energy dissipation mechanisms based on friction. *Soil Dyn. Earthq. Eng.* **2021**, *146*, 106746. [CrossRef]

66. Samanta, M.; Abishek, R.; Sawant, V. Investigation on Axial Response of Pile Due to Staged Tunnelling: A Numerical Approach. In *Stability of Slopes and Underground Excavations*; Springer: Berlin/Heidelberg, Germany, 2022; pp. 267–278.

67. Li, L.; Zheng, M.; Liu, X.; Wu, W.; Liu, H.; El Naggar, M.H.; Jiang, G. Numerical analysis of the cyclic loading behavior of monopile and hybrid pile foundation. *Comput. Geotech.* **2022**, *144*, 104635. [CrossRef]

68. Chen, H.; Zhang, L. A Machine Learning-Based Method for Predicting End-Bearing Capacity of Rock-Socketed Shafts. *Rock Mech. Rock Eng.* **2022**, *55*, 1743–1757. [CrossRef]

69. Liang, S.; Foong, L.K.; Lyu, Z. Determination of the friction capacity of driven piles using three sophisticated search schemes. *Eng. Comput.* **2020**, *38*, 1515–1527. [CrossRef]